Numerical calculation of magnetization behavior for Co nanowire array

ZHONG Ke-hua(钟克华), HUANG Zhi-gao(黄志高), CHEN Zhi-gao(陈志高),
FENG Qian(冯 倩), YANG Yan-min(杨艳敏)

Department of Physics, Fujian Normal University, Fuzhou 350007, China

Abstract: Based on Monte Carlo method, the hysteresis loops for both individual Co nanowires and their array were simulated, and the influence of the strength of the dipolar interaction on the macroscopical magnetic properties of Co nanowire array was investigated. The simulated results indicate that the coercivity approximately increases linearly with the increase of the strength coefficient of the dipolar interaction. The interwire dipole interaction between wires tends to develop a magnetic easy axis perpendicular to the wire axis. In the magnetic reversal process, competition between the interwire dipolar interaction and the shape anisotropy of individual wires which forces the moments to orient along the axis makes the magnetic reversal of the array different from that of individual wire. For applied field parallel to wire axis, the coercivity of nanowire array increases rapidly with the increase of the nearest-neighbor interwire distance, and approximately increases linearly with the increase of the strength coefficient of the dipolar interaction for the fixed diameter and the nearest-neighbor interwire distance. While for applied field perpendicular to wire axis, in contrast, the coercivity decreases with increasing the nearest-neighbor interwire distance, and nearly remains a constant with the increase of the strength coefficient of the dipolar interaction.

Key words: Co nanowires; interwire dipole interaction; Monte Carlo method

1 Introduction

Because of their potential application in ultrahigh density magnetic recording media[1], the nanostructured magnetic elements such as regular arrays of nanowires and nanodots are of interest not only in fundamental research[2−4] but also in the commercial preparation of the nanowires[5−7]. Nanowire arrays such as Fe, Co, Ni, and their alloys can been produced by electrodeposition in self-assembled anodic aluminium oxide templates. And many interesting properties, such as high coercivity and perpendicular magnetic anisotropy, have been found[8−14]. It is already well known that the magnetostatic interaction among wires can strongly affect the macroscopic magnetic properties of nanowire array. However, previously, more investigations were performed on understanding the magnetic reversal mechanisms of individual wires and the influence of the dimension of the wires on their magnetic properties, and few researches on the magnetostatic interaction among nanowires were conducted. The problem becomes quite complex when the magnetostatic interaction among wires is considered. Several models have been suggested as follows[3,15−18]: 1) a strong simplification on the magnetostatic interactions among nanowires was used to reduce the computational complexity, and the simulated results were only in qualitative agreement with the experiment facts [3]; 2) a comparatively small number of nanowires were studied[15]; 3) the magnetostatic interaction among nanowires was omitted. Up to date, as the system of magnetic nanowires is very complex, the problem regarding the influence of the magnetostatic interaction among nanowires in the close-packed arrays on the magnetic properties is still unsolved. In this work, based on the Monte Carlo simulation, the hysteresis loops for both individual Co nanowires and their array were simulated, and the influence of the strength of the dipolar interaction on the macroscopical magnetic properties was investigated. Simultaneously, the magnetic reversal processes of individual wires and nanowire array were discussed.

2 Modeling and method

Assuming R_w/d_w denotes the ratio of center-to-center spacing between the nearest-neighbor nanowires and the diameter of the wire (d_w is the diameter of the wire, R_w is center-to-center spacing among the nearest-neighbor nanowires), the following model was chosen for the simulation.

1) The geometry of all nanowires is absolutely uniform and parallel to each other strictly, and the aspect ratio l_w/d_w of the wire is 10:1 (where l_w is the length).

2) A 6×6 two-dimensional hexagonal array with periodic boundary conditions was used for the simulation.

Fig.1 shows the schematic drawing of a top view of the array of nanowires used in the simulation. The magnetic hysteresis loops and magnetization curves were simulated with Monte Carlo method and the detailed descriptions can be found in Refs.[19−22]. For the calculation, the finite element algorithm was used. The discretization element was regular global-shaped cell (sphere). The total energy of the nanowire array was given by

$$E = -\sum_{<ij>} J\boldsymbol{S}_i\boldsymbol{S}_j + D\sum_{i<j}\left[\frac{\boldsymbol{S}_i\boldsymbol{S}_j}{r_{ij}^3} - 3\frac{\boldsymbol{S}_i\boldsymbol{r}_{ij}\cdot\boldsymbol{S}_j\boldsymbol{r}_{ij}}{r_{ij}^5}\right] - M_s v_0 H\sum_i \boldsymbol{S}_i\boldsymbol{h} \tag{1}$$

The first term is the exchange of interaction energy, where $J=2Ad\pi/6$; d is the diameter of the sphere, and A is the exchange of coupling between spheres (within each sphere the magnetization is taken uniform). The second term represents the dipolar interaction of the nanowires in the array, where $D=P(M_s v_0)^2$ (M_s is saturation magnetization) denotes the strength of the dipole-dipole interaction; $v_0=\pi d^3/6$ is the volume of the sphere; P is the coefficient of the strength of the dipole-dipole interaction; r_{ij} is the vector for the displacement between sites i and j. The last term represents Zeeman energy. $H\boldsymbol{h}$ is the applied field. Due to that the emphases is to consider the influence of the dipolar interaction, the magnetocrystalline anisotropy is ignored here. Because the calculation of the dipolar interaction is the long-range interaction, it is very time-consuming. Fortunately, the dipolar interaction inverses three cubed of their distance, so it will be ingored when their distance is so far. In former literature, to save time, the interactional spins are commonly considered within a sphere whose centre locates in the position of the spin considered and the radius of the sphere R_0 is generally assumed six multiple of parameter a which is the distance between two nearest-neighbor spins[23−24]. However, to study the interaction among the nanowires in this work, the radius
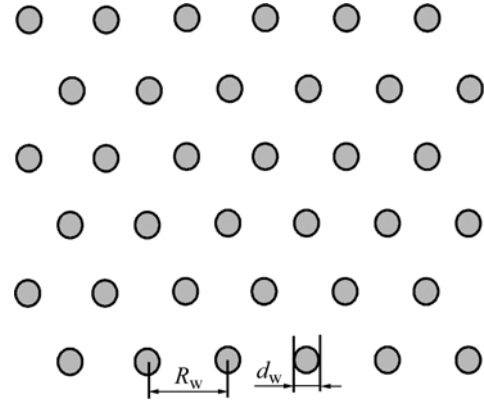

Fig.1 Schematic drawing of top view of hexagonal array of nanowires used in calculation (a circle represents a nanowire)

of the sphere R_0 is assumed as $25a$. For Co nanowires, the typical material parameters usually used in the simulation[25] is given by $A=1.3\times10^{-11}$ J/m, $M_s=1.43\times10^6$ A/M.

3 Results and discussion
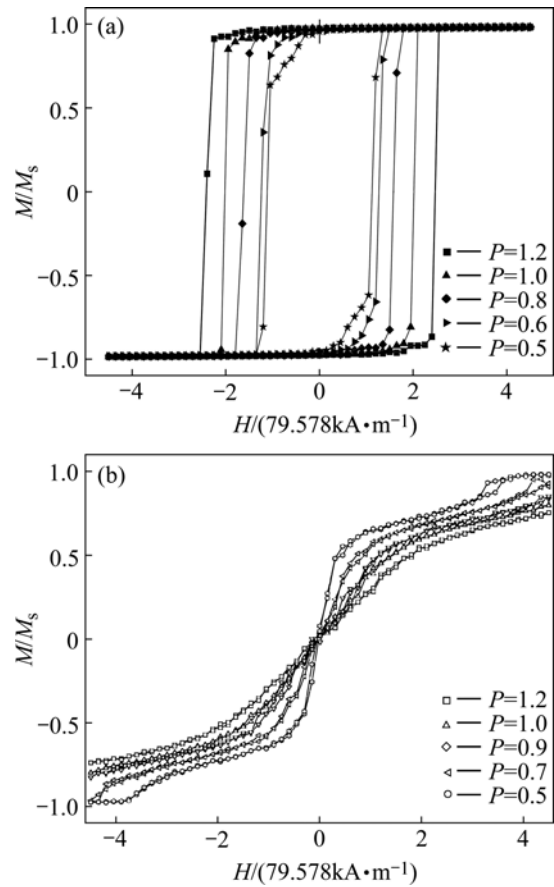
Figs.2(a) and (b) show the normalized magnetic

Fig.2 Normalized magnetic hysteresis loops for Co individual nanowire for various ratios P for applied field parallel(a) and perpendicular(b) to wires axis

hysteresis loops $M(H)$ of the individual Co nanowire for various coefficient P. From Fig.2, it is found that the easy axis loops (the applied field is parallel to the wire axis) of the individual wire are along the wire axis, which results mainly from the shape anisotropy of the nanowire. For the easy axis loops, the squareness and coercivity increase with the increase of coefficient P. For the hard axis loops (the applied field is perpendicular to the wire axis) the coercivity are nearly zero, and the loops slant flatly while the coefficient P increases. This causes the increase of the saturation field. Fig.3 shows the dependence of the coercivity on the coefficient P corresponding to Fig.2(a). From Fig.3, it is observed that the coercivity H_c increases almost linearly with the increase of the strength coefficient of the dipolar interaction.
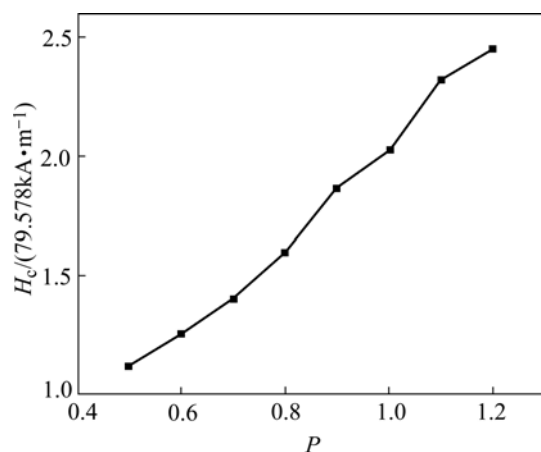

Fig.3 Dependence of coercivity on strength coefficient of dipolar interaction for applied field parallel to wire axis

In the following, we investigate the influence of interwire dipolar interaction on the macroscopical magnetic properties of Co nanowire array. Fig.4 shows the normalized magnetic hysteresis loops $M(H)$ of the individual Co nanowire and the hexagonal-close-packed nanowire array. The ratio R_w/d_w of the nanowire array is 4/3 (R_w is the distance among the nearest-neighbor nanowires, d_w is the diameter of the nanowires), and the coefficient of the strength of the dipole-dipole interaction $P=1.0$. $H(//)$ and $H(\perp)$ denote the applied field is parallel and perpendicular to the wires axis, respectively. From Fig.4, it is found that for the applied field parallel to the wire axis, the easy axis loop of the wires array slants, and the squareness and coercivity decrease markedly compared with those of the individual wire. These results are consistent with other investigator's experimental and calculational results[15,26−29]. The squareness and coercivity in the hard axis loops of nanowire array are evidently increased under the role of the interwire dipole

interaction among wires, while they are nearly zero for the individual wire. It is implied that the magnetostatic coupling among wires tends to develop a magnetic easy axis perpendicular to the wire axis. This is consistent with the experimental results[18].
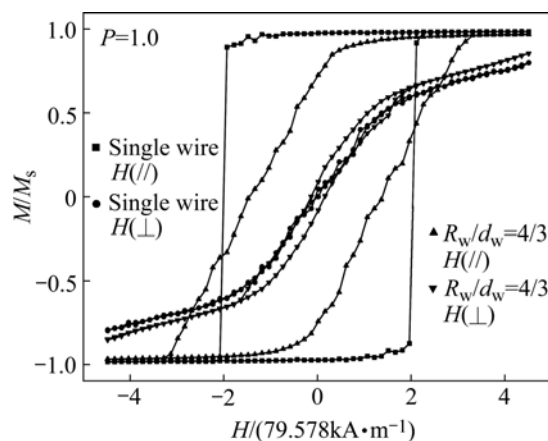

Fig.4 Normalized magnetic hysteresis loops of individual Co nanowire and array with $R_w/d_w= 4/3$

It is well known that magnetic reversal mechanisms play an important role in explaining magnetic properties of the nanowires, and they have been discussed in the last decade. To get a comprehension of the magnetic reversal mechanisms of Co nanowires profoundly, the configurations during the reversal process are shown in Fig.5. Fig.5(a) shows the reversal process corresponding to different magnetization levels of the individual nanowire. For very thin individual nanowire, the reversal mechanism is mainly described by a nucleation-propagation process, which starts at the ends of the nanowire. As the external field with the sufficient strength is applied parallel to the nanowire axis, all moments in the nanowire are forced to be parallel to the direction of the external field. When the external field decreases to zero, subsequently, the external field with opposite orientation reaches to the nucleation field, and the moments at the end of the nanowire rotate out of the axis and finally reverse. But, at the same time, the rest moments of the sample remain mostly homogeneously magnetized antiparallel to the field. The reversal at one end of the sample leads to the formation of a soliton. Then it propagates through the nanowire, and a complete reverse of moment is finished. Fig.5(b) shows the magnetization states of the several nanowires of the 6×6 two-dimensional hexagonal array after saturation and subsequent application of a reversed field H=1 650 (79.578 A·m⁻¹). In the nanowire array, the shape anisotropy of the nanowire impels the easy axis along the wires axis, whereas the interwire dipole interaction
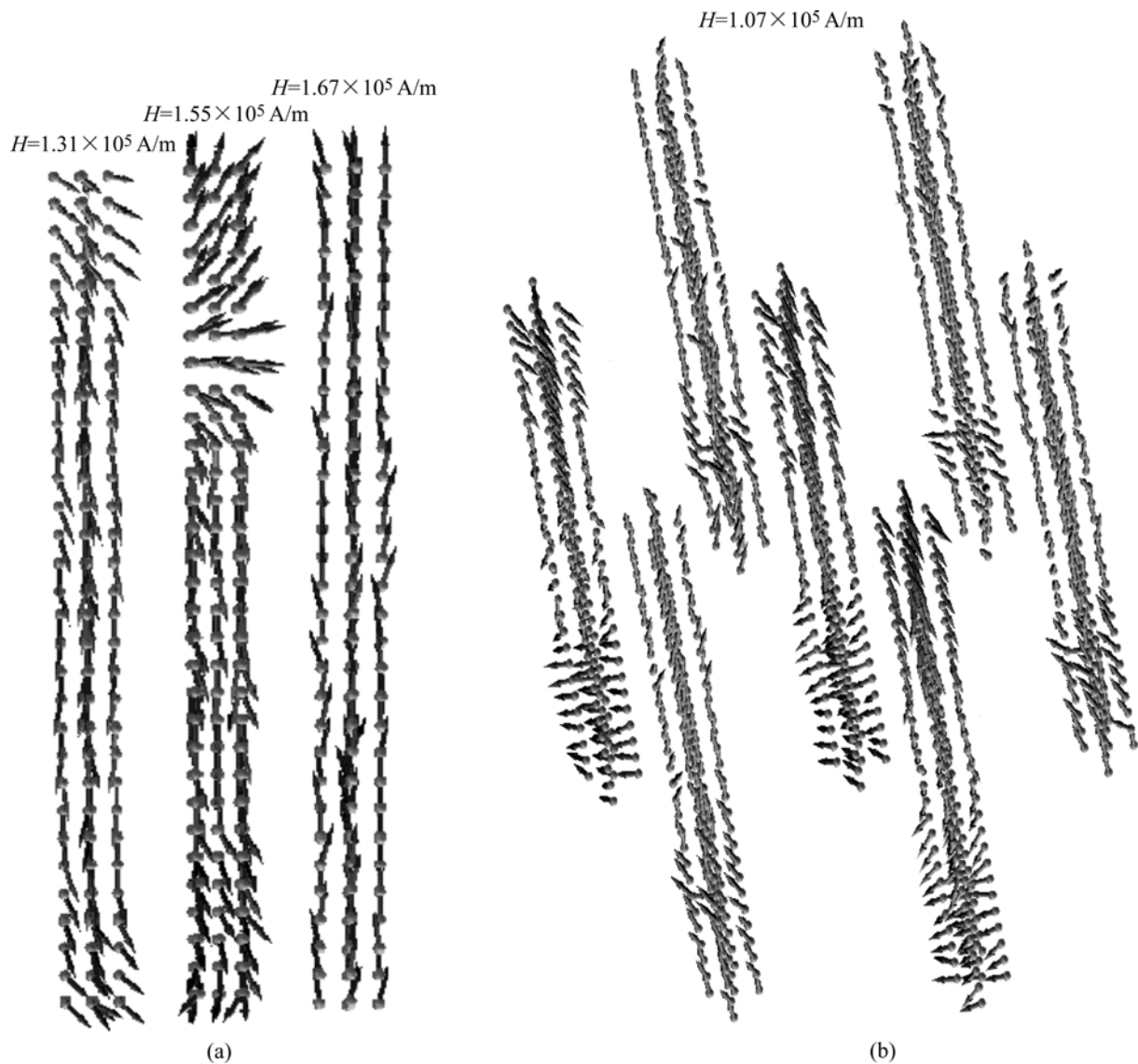
Fig.5 Magnetization reversal of individual nanowire (a) and that of seven nanowires in 6×6 two-dimensional hexagonal array (b) (Here, applied field is parallel to axis of nanowire)

among wires impels the easy axis perpendicular to wires axis. Then they compete with each other in the magnetic reversal process. As a result, the magnetic reversal mechanism is different from that of individual wire. As shown in Fig5(b), some nanowires switch in the direction of the external field, while the others remain homogeneously magnetized antiparallel to the field. This denotes that this external field is not enough to switch the whole nanowire array. The reversal of some nanowires occurs because the stray field of neighboring nanowires adds to the external field and leads to a higher field to which the magnetic moments are effectively exposed. In this way, the moment reversal of some nanowires firstly occurs; however, those reversed nanowires will produce a stray field opposite to the external field and reduce the local field, so they need the

higher external field to realize reversal. With increasing external field, those non-reversed nanowires will produce gradually reversal, and ultimately the reversal of the whole wires array is finished. Thus, in the first process, the total magnetizations of the array are smaller. This is similar to the simulated results in Ref. [15].

Figs.6(a) and (b) show the normalized magnetic hysteresis loops $M(H)$ of the individual nanowire and wire array with d_w=15 nm, R_w/d_w=3.5/3, 4/3, 5/3, 3, 4, and P= 1.0. From Fig.6, it is found that, for the applied field parallel to the wires axis, with increasing value of R_w, the squareness and coercivity are enhanced. As the value of R_w/d_w is large enough, such as R_w/d_w=4, the hysteresis loop is close to that of individual wire. For the applied field perpendicular to the wires axis, with the increase of R_w, the changes of hysteresis loops are not
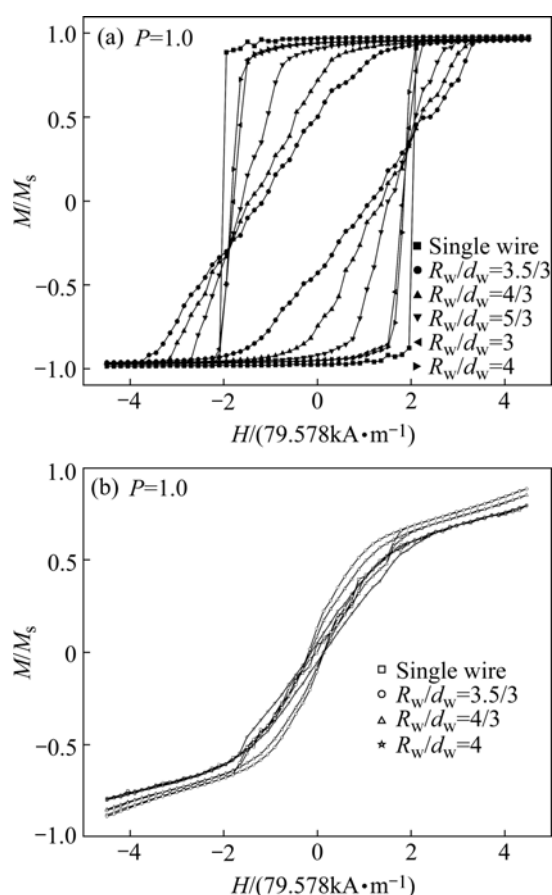
Fig.6 Normalized magnetic hysteresis loops of Co individual nanowire and wires array with d_w=15 nm and R_w/d_w=3.5/3, 4/3, 5/3, 3, 4 for $H(//)$ (a) and $H(\perp)$ (b)

obvious. But, the change trend opposes to the case of the applied field parallel to wires axis.

The change of the magnetic hysteresis loops can be explained as follows: 1) In the reversal process, when the applied field is parallel to wires axis, due to the fact that the interwire dipole interaction among wires favors the moment to be perpendicular to wires axis, it competes with the shape anisotropy of the nanowire which impels the magnetization to align along the wire axis. Consequently, the stray field along nanowire axis reduces, so it causes smaller squareness and coercivity of hysteresis loops. The dipolar interaction inverses three cubed of their distance R_w, therefore, its influence on the magnetic properties of nanowire array is reduced very rapidly with increasing the distance between nanowires. When R_w/d_w=4, the dipolar interaction is so little that it can be ignored, so the hysteresis loop of array is close to that of individual nanowire, as shown in Fig.6(a). 2) When the applied field is perpendicular to the wire axis, since the dipolar interaction among wires impels the magnetization to align perpendicular to wire axis, it gives rise to the stray field perpendicular to the wires axis.

However, compared with the shape anisotropy of nanowires, the dipolar interaction among wires is still weak, even for the close-packed nanowire array such as R_w/d_w=3.5/3. Therefore, the coercivity is very small compared with the case of the applied field parallel to wire axis. To observe clearly, Figs.7(a) and (b) show the coercivity as a function of the ratio R_w/d_w for $H(//)$ and $H(\perp)$, respectively. As shown in Fig.7(a), for smaller ratio R_w/d_w (about $3.5/3 < R_w/d_w < 7/3$), the coercivity H_c for $H(//)$ increases rapidly with increasing ratio R_w/d_w, while for larger ratio R_w/d_w (about $7/3 < R_w/d_w < 4$), the coercivity increases slowly. As seen from Fig.7(b), the coercivity for $H(\perp)$ decreases generally with the increase of ratio R_w/d_w, which is contrary to the case of Fig.7(a).
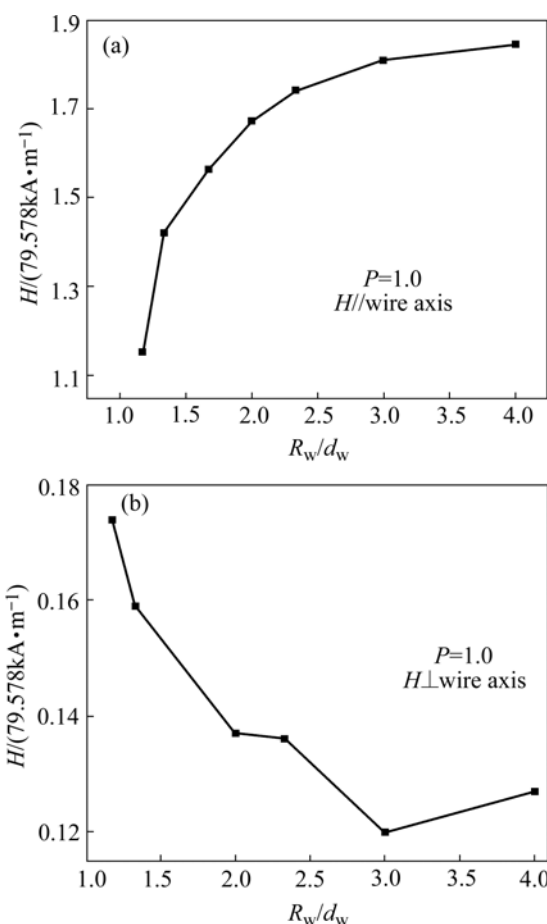

Fig.7 Dependence of coercivity on ratio R_w/d_w for Co nanowire array with d_w=15 nm

Simultaneously, we study the influence of the strength of the dipolar interaction on the macroscopical magnetic properties of nanowire array. Fig.8 shows the coercivity as a function of the strength coefficient of interwire dipolar interaction P for Co nanowire array with d_w=15 nm, R_w/d_w=4/3, both $H(//)$ and $H(\perp)$ cases, respectively. It can been seen from the figure, for $H(//)$, the coercivity approximately increases linearly with the

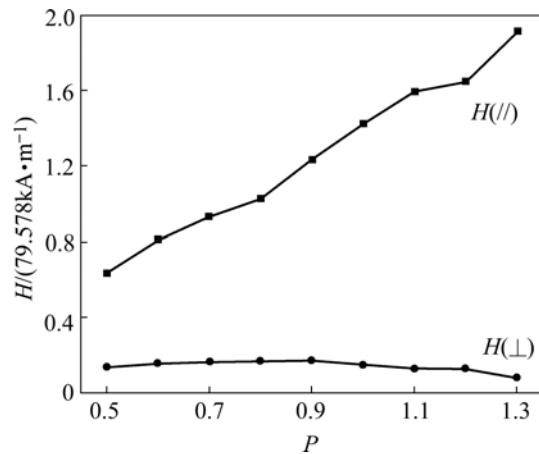increase of the strength coefficient P. However, for $H(\perp)$, the coercivity remains nearly unchanged.

Fig.8 Coercivity as function of strength coefficient of interwire dipolar interaction P for Co nanowires array with d_w=15 nm, R_w/d_w=4/3, both $H(//)$ and $H(\perp)$ cases

4 Conclusions

1) For individual nanowire, with the increase of the strength coefficient of the dipolar interaction, the coercivity approximately increases linearly and the shape anisotropy of nanowire increases.

2) For the nanowire array, the interwire dipolar interaction tends to develop a magnetic easy axis perpendicular to the nanowire axis. For the applied field parallel to the wire axis, the interwire dipolar interaction makes the hysteresis loops slant and the squareness and coercivity descend obviously. For the applied field perpendicular to wire axis, the interwire dipolar interaction has the coercivity and remanence enhance.

3) In the magnetic reversal process of the nanowire array, competition between the interwire dipolar interaction and the shape anisotropy of individual nanowire makes the magnetic reversal of the array different from that of individual wire. For wires array, the moment reversal of some nanowires firstly occurs, and others reverse gradually with increasing applied field and ultimately the reversal of the whole wires array is achieved.

4) When applied field is parallel to wire axis, for smaller ratio R_w/d_w (about $3.5/3 < R_w/d_w < 7/3$), the coercivity of nanowire array increases rapidly with the increase of the nearest-neighbor interwire distance, while for larger ratio R_w/d_w (about $7/3 < R_w/d_w < 4$), the coercivity increases slowly. And the coercivity approximately increases linearly with the increase of the strength coefficient of the dipolar interaction for the fixed diameter and nearest-neighbor interwire distance.

When the applied field is perpendicular to wire axis, in contrast, the coercivity decreases with increasing the nearest-neighbor interwire distance, and remains nearly unchanged with increasing strength coefficient of the dipolar interaction.

References

[1]   CHOU S Y. Pattered magnetic nanostructures and quantized magnetic disk [J]. Proceedings of the IEEE, 1997, 85: 652−671.

[2]   BENNETT A J, XU J M. Simulating the magnetic susceptibility of magnetic nanowire arrays [J]. Appl Phys Lett, 2003, 82: 3304−3306.

[3]   RAPOSO V, GARCIA J M, GONZALEZ J, VAZQUEZ M. Long-range magnetostatic interactions in arrays of nanowires [J]. J Magn Magn Mater, 2000, 222: 227−232.

[4]   GUSLIENKO K Y. Magnetostatic interdot coupling in two-dimensional magnetic dot arrays [J]. Appl Phys Lett, 1999, 75: 394−396.

[5]   CHENG G S, ZHANG L D, ZHU Y, FREI G T, LI L, MO C M, MAO Y Q. Large-scale synthesis of single crystalline gallium nitride nanowires [J]. Appl Phys Lett, 1999, 75: 2455−2457.

[6]   WANG X F, ZHANG L D, SHI H Z, PENG X S, ZHENG M J, CHEN J L, GAO B J. Ordered single-crystalline Bi nanowire arrays embedded in nanochannels of anodic alumina membranes [J]. J Phys D: Appl Phys, 2001, 34: 418−421.

[7]   LI Y, MENG G W, ZHANG L D, PHILIPP F. Ordered semiconductor ZnO nanowire arrays and their photoluminescence properties [J]. Appl Phys Lett, 2000, 76: 2011−2013.

[8]   SKOMSKI R, ZENG H, SELLMYER D J. Magnetic localization in transition-metal nanowires [J]. Phys Rev B, 2000, 62: 3900−3904.

[9]   VELAZQUEZ J, GARCIA C, VAZQUEZ M, HERNANDO A. Interacting amorphous ferromagnetic wires: A complex system [J]. J Appl Phys, 1999, 85: 2768−2774.

[10]   SAMPAIO L C, SINNECKER E H C P, CERNICCHIARO G R C, KNOBEL M, VAZQUEZ M, VELAZQUEZ J. Magnetic microwires as macrospins in a long-range dipole-dipole interaction [J]. Phys Rev B, 2000, 61: 8976−8983.

[11]   BELLIARD L, MILTAT J, THIAVILLE A, DUBOIS S, DUVAIL J, PIRAUX L. Observing magnetic nanowires by means of magnetic force microscopy [J]. J Magn Magn Mater, 1998, 190: 1−16.

[12]   FERT A, PIRAUX L. Magnetic nanowires [J]. J Magn Magn Mater, 1999, 200: 338−358.

[13]   PAULUS P M, DE JONGH L J, PAULUS P M, LUIS F, KROLL M, SCHMID G. Low-temperature study of the magnetization reversal and magnetic anisotropy of Fe, Ni, and Co nanowires [J]. J Magn Magn Mater, 2001, 224 : 180−196.

[14]   ZHANG X Y, WANG G H, CHAN Y F, ZHENG P K, ZHANG X X, WANG N. Fabrication and magnetic properties of ultrathin Fe nanowire arrays [J]. Appl Phys Lett, 2003, 83: 3341−3343.

[15]   HERTEL R. Micromagnetic simulations of magnetostatically coupled Nickel nanowires [J]. J Appl Phys, 2001, 90: 5752−5758.

[16]   FODOR P S, TSOI G M, WENGER L E. Fabrication and characterization of $Co_{1-x}Fe_x$ alloy nanowires [J]. J Appl Phys, 2002, 91: 8186−8188.

[17]   LOPEZ-URIAS F, MUNOZ-SANDOVAL E, REYES-REYES M, ROMERO A H, TERRONES M, MORAN-LOPEZ J L. Creation of helical vortices during magnetization of aligned carbon nanotubes filled with Fe: Theory and experiment [J]. Phys Rev Lett, 2005, 94: 216102−216105.

[18] VAZQUEZ M, HERNANDEZ-VELEZ M, PIROTA K, ASENJO A, NAVAS D, VELAZQUEZ J, VARGAS P, RAMOS C. Arrays of Ni nanowires in alumina membranes: Magnetic properties and spatial ordering [J]. Eur Phys J B, 2004, 40: 489−497.

[19] BINDER K, HEERMANN D W. Monte Carlo simulation in statistical physics [M]. Berlin: Springer, 1992.

[20] HUANG Z G, CHEN Z G, PENG K, WANG D H, ZHANG F M, ZHANG W Y, DU Y W. Monte Carlo simulation of tunneling magnetoresistance in nanostructured materials [J]. Phys Rev B, 2004, 69: 094420−094426.

[21] HUANG Z G, CHEN Z G, ZHANG F M, DU Y W. Magnetization and configurational anisotropy in magnetic clusters: Monte Carlo simulation [J]. Eur Phys J B, 2004, 37: 177−185.

[22] YANG Y M, ZHONG K H, FENG Q, JIANG L Q, HUANG Z G. Monte Carlo simulation of Kerr effect and giant magnetoresistance in Co_xAg_{1-x} granular films [J]. Chin Phys Lett, 2005, 22: 1305−1308.

[23] ZHU J G, BERTRAM H N. Micromagnetic studies of thin metallic films (invited) [J]. J Appl Phys, 1988, 63(4): 3248−3253.

[24] WENG Zhen-zhen, FENG Qian, HUANG Zhi-gao, DU You-wei. Study on the coercivity and step effect of mixed magnetic films by micromagnetism and Monte Carlo simulation [J]. Acta Physica Sinica 2004, 53: 3177−3185.

[25] HAUSMANNS B, KROME T P, DUMPICH G, WASSER MANN E F, HINIKE D, NDWAK U, USADEL K D. Magnetization reversal process in thin Co nanowires [J]. J Magn Magn Mater, 2002, 240: 297−300.

[26] ABRAHAM M C, SCHMIDT H, SAVAS T A. Magnetic properties and interactions of single-domain nanomagnets in a periodic array [J]. J Appl Phys, 2001, 89(10): 5667−5670.

[27] TSUYA N, SAITO Y, TOKUSHIMA T. A perpendicular magnetic recording medium by alumite [J]. J Magn Magn Mater, 1986, 54/57: 1681−1682.

[28] MIYASHITA E, KUGA K. Simulation of magnetization patterns of perpendicular media for ultra-high recording density [J]. J Magn Magn Mater, 2001, 235: 413−417.

[29] TAYACKA A, YAMASAKI J. Preparation of Co-Fe-P amorphous fine needles with anodization technique and measurement of demagnetizing factor [J]. J Appl Phys, 1996, 79(8): 6016−6018.

(Edited by LI Xiang-qun)